

DOI 10.24425/aee.2020.133030

## Research on beam supply control strategy based on sliding mode control

HAO ZHANG , HAIYING DONG, BAOPING ZHANG, TONG WU, CHANGWEN CHEN

Lanzhou Jiaotong University  
China

Lanzhou Institute of Physics  
China  
e-mail: zhanghao6665@163.com

(Received: 11.09.2019, revised: 08.01.2020)

**Abstract:** In the hybrid multiple H-bridge topology of beam supply, the load change of a DC/DC full-bridge converter can greatly affect the output voltage during onsite operation. An improved sliding mode control (SMC) strategy is thus proposed in this paper, where the rate of switching control is added to the law of system equivalent control to create a law that can realize a complete sliding mode control. Considering the special operating conditions of the load can have an influence on the performance of the controller, the impact of uncertainty existing in onsite conditions is suppressed with the proposed strategy utilized. The validity of the proposed strategy, finally, is verified by simulation, which proves the outperformance of the system in both robustness and dynamics.

**Key words:** beam supply, DC/DC converter, robustness, sliding mode control

### 1. Introduction

With the rapid development of high-power ion-electric propulsion technology in China, the power level of the power processing unit (PPU) of the ion thruster is getting higher and higher, and the high-efficiency, high-density beam supply has become the development direction of the PPU. The beam supply is the core component of the PPU. Therefore, designing a suitable beam supply is the key to achieving a high-efficiency and high-power ion PPU. It's of great significance to study the control of beam supply for the rapid development of high-power ion-electric propulsion technology in China [1–2].



© 2020. The Author(s). This is an open-access article distributed under the terms of the Creative Commons Attribution-NonCommercial-NoDerivatives License (CC BY-NC-ND 4.0, <https://creativecommons.org/licenses/by-nc-nd/4.0/>), which permits use, distribution, and reproduction in any medium, provided that the Article is properly cited, the use is non-commercial, and no modifications or adaptations are made.

At present, the beam supply usually adopts a phase-shifted dual-bridge converter structure, and scholars mainly focus on the transformation of circuit topology structure [3–4]. For the design of a beam controller, the classical PID control theory method of voltage and current multiple closed loop is usually adopted [5]. In the actual engineering control of the beam supply, the robustness and dynamic performance are poor. Sliding mode control (SMC) has the advantages of fast dynamic response and simple application, especially suitable for variable structure systems with strong robustness and fast dynamic response. The difference between the SMC and the traditional PID control method lies in the discontinuity of the SMC. The principle is to guide the state trajectory of the system at any time to a preset slip under the action of a continuously switching control law. When the state trajectory of the system reaches the sliding mode switching surface, it will be limited to the sliding surface and converge to the equilibrium point for a limited time. The beam supply phase-shift full-bridge converter continuously switches the on and off states of the switch tube, which is a strictly variable structure system and highly compatible with the principle of sliding mode variable structure control. The literature [6] proposed the control strategy of the sliding mode controller, so that the system has good response speed. The literature [7] proposed a full-order sliding mode control strategy to track the output voltage, which is robust to the uncertainties of the system and has a good transient response. In [8], the voltage control mode, current control mode and the SMC mode were compared to obtain the strong nonlinear characteristics of SMC. In [9], an indirect multiple-loop sliding mode control method was proposed for boost circuits. In [10], a hysteresis-based SMC method was proposed, and the relationship between the switching frequency of the buck converter and the hysteresis width is derived.

After the traditional control is designed, the parameters are fixed and the adaptability is poor. In the actual system, the system status and parameters change randomly/frequently/largely, reflecting the uncertainty of the power system. It is difficult for the controller to achieve the best control effect. Sliding mode control can overcome the uncertainty of the controlled system, especially for the interference dynamics. Moreover, for the SMC of the DC/DC switching power supply, the method proposed in the above literature is rarely involved in the full-bridge conversion circuit, and the problem of the influence of the load variation on the output voltage is not solved.

This paper proposes an improved SMC control strategy to achieve automatic tracking of the reference voltage. It has better anti-interference ability, ensuring the system has good dynamic characteristics and strong robustness. Firstly, for the dual-mode control system of beam supply, a new type of beam supply topology of a hybrid multiple H-bridge is designed. Secondly, the small-signal model is established to obtain the system state-space equation. Then, based on the equivalent control law of the system, the switching control rate is added to form a complete SMC law. Finally, the effectiveness of the proposed method is verified by comparing it with the traditional PID control under abnormal conditions.

## 2. Converter topology and working principle

### 2.1. Topology of the converter

For the new beam supply topology, as shown in Fig. 1, the switch tubes  $A_1$ – $A_4$ ,  $B_1$ – $B_4$  form a new hybrid multiple H-bridge structures, the inductor  $L_f$  and the capacitor  $C_f$  form an

output filter network,  $V_o$  is the output voltage of the load, diodes  $D_1$ ,  $D_2$  and  $D_3$  constitute a secondary side rectifier bridge. The primary and secondary side transformation ratios of the isolation transformers  $T_1$  and  $T_2$  are  $K = 1:10$ , this structure can effectively reduce the current and voltage stress of the switch tube, and can solve a wide range of output voltage problems.

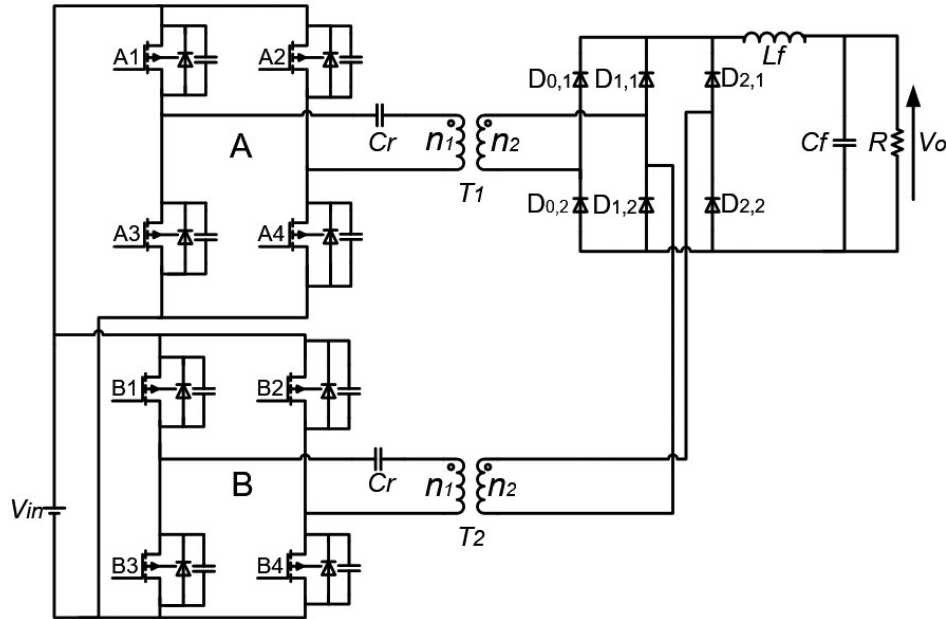


Fig. 1. New full-bridge converter circuit topology

## 2.2. Working principle

First assume that all switches and diodes are ideal, and each transformer has the same turns ratio. The system has the following modes:

Mode 1:  $A_1$ ,  $A_4$ , and  $B_1$ ,  $B_4$  are turned on, the input voltage begins to shift to the corresponding secondary side, becoming  $T'_1$  and  $T'_2$ ; the primary currents  $I_{P1}$  and  $I_{P2}$  of  $T_1$  and  $T_2$  increase linearly, as shown in Fig. 2, diodes  $D_{0,1}$ ,  $D_{1,1}$  and  $D_{1,2}$ ,  $D_{2,2}$  are turned on.  $D_{1,1}$  participates in power conversion to the anode voltage above the cathode voltage of  $D_{1,1}$ , which causes the diode to reverse block. When  $T'_1$  and  $T'_2$  in the in-series mode as well as,  $D_1$  paths are not conducting, then the final output voltages are 2 times of  $T'_1$  rectified, and it is denoted as  $2V_o$ .

Mode 2: mode 1 lasts for a short time. When  $D_{1,1}$  and  $D_{1,2}$  are off,  $D_{0,1}$  and  $D_{2,2}$  are still on,  $I_{P1}$  and  $I_{P2}$  keep increasing, and the output voltage  $V_o$  is  $T'_1$  and  $T'_2$  at this moment. The sum is shown in Fig. 3.

$$I_{p1} = I_{p2} = \frac{I_o}{k} + \frac{V_{in}}{L_f}, \quad V_o = V_{sec1} + V_{sec2} - V_{D_{0,1}} - V_{D_{2,2}} = 2(V_{sec1} - V_{D_{0,1}}), \quad (1)$$

where  $V_{in}$  is the input voltage of the converter and  $V_o$  is the output voltage;  $V_{p1}$  and  $V_{p2}$  are the voltages of the secondary sides  $T'_1$  and  $T'_2$ , respectively.  $V_{D_{0,1}}$ ,  $V_{D_{0,2}}$ ,  $V_{D_{1,1}}$ ,  $V_{D_{1,2}}$ ,  $V_{D_{2,1}}$  are the turn-on voltages of the rectifier diodes.

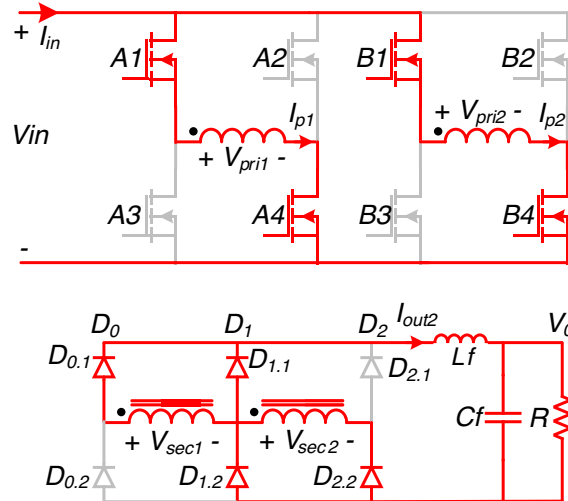


Fig. 2. Linear increase in  $I_{P1}$  and  $I_{P2}$

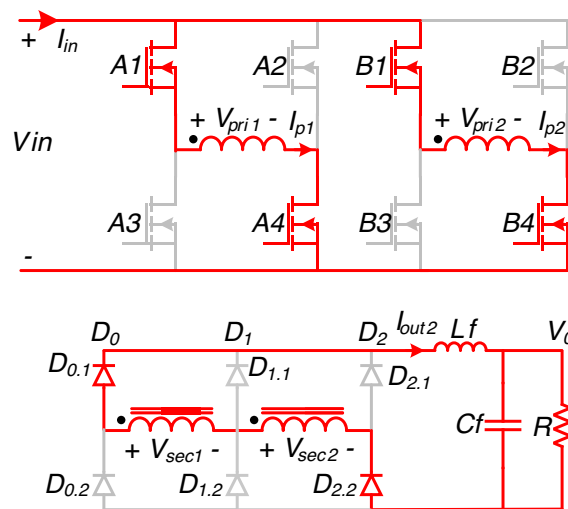


Fig. 3. Mode 2 process diagram

Mode 3: when  $A_1, A_4$  are closed and  $B_1, B_4$  are still open, the primary side current of transformer  $T_1$  begins to decrease, and the inductance of the resonant tank transformer generated by the primary side leakage inductance is expressed as  $L_{lk}$ , the capacitance of parasitic resistance  $A_1, A_4$  as  $C_{oss}$ . When  $V_{sec2}$  remains unchanged,  $V_{sec1}$  will decrease from  $kV_s$  to  $V_{D_{0,1}}$ , less than  $V_{sec2}$ , causing diodes  $D_{0,1}$  and  $D_{1,2}$  turned off,  $D_{1,1}$  and  $D_{2,2}$  to be turned on, as shown in Fig. 4.

$$V_{C_{oss}} = kI_o Z_o \sin \omega_o(t - t_3), \quad (2)$$

where

$$\omega_o = \frac{1}{\sqrt{2L_f C_{oss}}}, \quad Z_o = \sqrt{\frac{L_f}{2C_{oss}}}$$

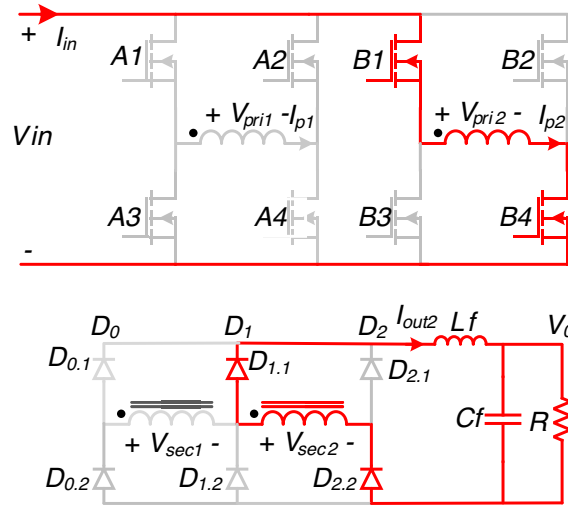


Fig. 4. Mode 3 process diagram

Mode 4: as the phase-shift angle increases, the operating mode of the system changes from series mode to parallel mode. The  $B_1$ ,  $B_4$ ,  $A_2$ , and  $A_3$  switches open and increase in the opposite direction.  $T'_1$  and  $T'_2$  are equivalent to parallel. The current stress of  $D_{1,1}$  is twice that of  $D_{0,2}$  or  $D_{2,2}$ , and the output voltage is determined by  $T'_1$  and  $T'_2$ , as shown in Fig. 5.

$$I_{p1} = -I_{p2} = \frac{I_o}{2k} + \frac{V_{in}}{L_f}, \quad V_o = V_{sec1} - V_{D_{0,2}} - V_{D_{1,1}} = kV_{pri1} - 2V_{D_{1,1}} \quad (3)$$

Mode 5: the leakage inductance of transformer  $T_1$  is the same as  $T_2$ , and the current flow through the resonant circuit to drop mode 3. The other modes apply the same operating procedure from mode 1 to 4, but with opposite phase directions. By analyzing mode 2 and 4, indicating different phase-shift angles, the output voltage  $V_o$  is from  $(kV_{pri1} - 2V_{D_{0,1}})$  to  $(2kV_{pri1})$ . We assume that  $V_{D_{0,1}}$  is zero, then the maximum value of the output voltage is twice the minimum value. Therefore, for the new full-bridge topology, the relationship between  $V_{in}$  and  $V_o$  can be expressed as:

$$M(D) = \frac{V_o}{V_{in}} = 2kD, \quad D = (T_s - 2T_{dead} - T_\theta) / T_s \quad (4)$$

where,  $T_{dead}$  is the dead time between  $A_1$  and  $A_2$ .  $T_\theta$  is the time of phase-shifted angle.

According to the working principle analysis, the system has two output states, the input parallel output series mode (phase-shift mode) and the input parallel output parallel mode (duty ratio mode), so that the system has flexible wide-range voltage output.

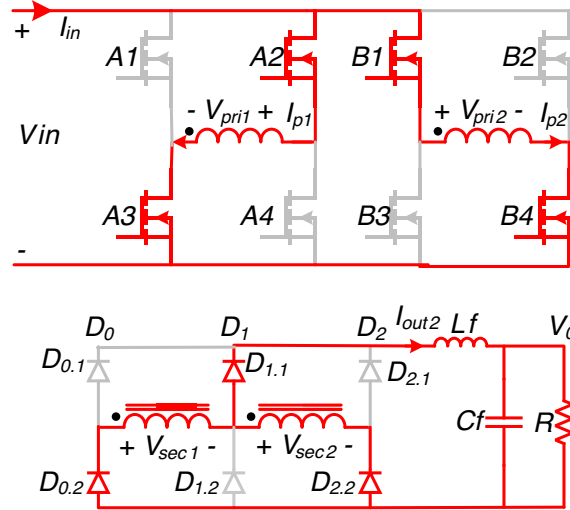


Fig. 5. Mode 4 process diagram

### 2.3. Small-signal modeling

When in the entire dynamic range of the beam DC/DC full-bridge converter. If the range of the signal is limited to a relatively small and approximately linear range in the entire dynamic range, the stripping DC bias takes its differential characteristics, resulting in an approximately linear model that facilitates system modeling analysis and design. For mode 2 and Fig. 6, the system is in series operation to establish a small-signal model.

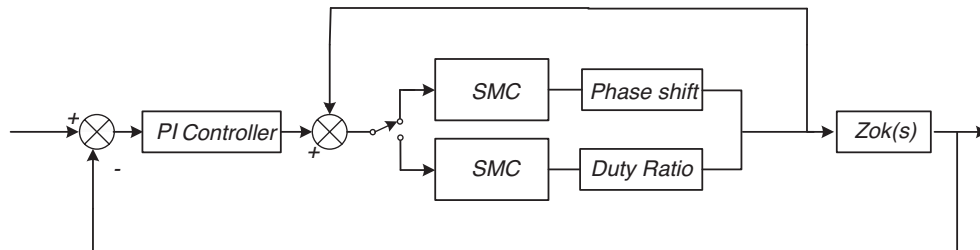


Fig. 6. Control system structure

The output filter circuit transfer function is:

$$H_o = \frac{\hat{v}_{out}(s)}{\hat{v}_o(s)} = \frac{1}{s^2 L_f C_f + s \frac{L_f}{R} + 1} \quad (5)$$

The input impedance  $z$  of the output filter is:

$$Z_f = sL_f + R \parallel \frac{1}{sC_f} = \frac{R}{1 + sL_f R} \left( s^2 L_f C_f + s \frac{L_f}{R} + 1 \right) = \frac{R}{1 + sL_f R} \frac{1}{H_o(s)} \quad (6)$$

From the small signal modeling analysis, the main power circuit transfer function in the phase-shift control mode is obtained. Make  $\hat{v}_{in} = 0$ .

The transfer function of duty ratio  $\hat{d}$  to output voltage  $\hat{v}_{out}$  is:

$$G_{vd}(s) = \left. \frac{\hat{V}_{out}(s)}{\hat{d}(s)} \right|_{\hat{v}_{in}(s)=0} = \frac{V_{in}/K}{s^2 L_f C_f + s [L_f/R + R_d C_f] + 1}. \quad (7)$$

The transfer function of duty ratio  $\hat{d}$  to inductor current  $G_{id}(s)$  is:

$$G_{id}(s) = \left. \frac{\hat{i}_L(s)}{\hat{d}(s)} \right|_{\hat{v}_{in}(s)=0} = \frac{V_{in}}{K} \cdot \frac{1 + s C_f R}{s^2 L_f C_f R + s (L_f + C_f R_d R) + R + R_d}, \quad (8)$$

where:  $R_d = \frac{4L_r}{K^2 T_s}$ ,  $R_d$  is the equivalent resistance.  $L_r$  is the leakage inductance of the transformer.

For the beam converter [11, 12], the control variable  $x$  is expressed as:

$$x = \begin{bmatrix} \dot{x}_1 \\ \dot{x}_2 \\ \dot{x}_3 \end{bmatrix} = \begin{bmatrix} V_{ref} - \beta v_o \\ \frac{d(V_{ref} - \beta v_o)}{dt} \\ \int (V_{ref} - \beta v_o) dt \end{bmatrix}, \quad (9)$$

where:  $x_1$  is the voltage error,  $x_2$  is the rate of change of the voltage error,  $x_3$  is the integral of the voltage error,  $V_{ref}$  is the output voltage reference value,  $\beta v_o$  is the output voltage detection value.

Substituting Equation (7) into (9), the state space equation of the full bridge converter can be obtained:

$$x = \begin{bmatrix} \dot{x}_1 \\ \dot{x}_2 \\ \dot{x}_3 \end{bmatrix} = \begin{bmatrix} x_2 \\ -\frac{1}{L_f C_f} \left( \frac{R_d}{R} + 1 \right) x_1 - \frac{1}{L_f C_f} \left( \frac{L_f}{R} + R_d C_f \right) x_2 - \frac{n V_{in}}{L_f C_f} d + \frac{1}{L_f C_f} \left( \frac{R_d}{R} + 1 \right) V_{ref} \\ x_1 \end{bmatrix}, \quad (10)$$

where:  $V_{in}$  is the input voltage, which is converted into the standard form:

$$\dot{x} = Ax + Bu + D.$$

$$A = \begin{bmatrix} 0 & 1 & 0 \\ -\frac{1}{L_f C_f} \left( \frac{R_d}{R} + 1 \right) & -\frac{1}{L_f C_f} \left( \frac{L_f}{R} + R_d C_f \right) & 0 \\ 1 & 0 & 0 \end{bmatrix}, \quad \dot{x} = \begin{bmatrix} x_1 \\ x_2 \\ x_3 \end{bmatrix},$$

$$B = \begin{bmatrix} 0 \\ -\frac{n V_{in}}{L_f C_f} \\ 0 \end{bmatrix}, \quad u = d, \quad D = \begin{bmatrix} 0 \\ \frac{1}{L_f C_f} \left( \frac{R_d}{R} + 1 \right) V_{ref} \\ 0 \end{bmatrix}.$$

### 3. Sliding mode control strategy of converter

#### 3.1. Structure of the control system

In order to improve the robustness and dynamic performance of the new beam supply DC/DC converter system, and it has excellent anti-interference performance to the input voltage change or load change, it can adapt to stable working under multiple working conditions. The classical linear system regulation strategy is combined with the sliding mode variable structure control strategy. The voltage and current multiple closed-loop control strategy can effectively solve the steady-state error and capacitor current detection in the SMC DC/DC converter. There are also other issues. The basic control principle is shown in Fig. 6. The outer loop is a voltage loop and the inner loop is a current regulation loop. The SMC is used to control the inductor current of the dual bridge circuit. The output of the voltage loop acts as an input to the current inner loop SMC, which in turn increases the effectiveness of the control strategy.

The current inner loop control is adopted, and the system has the inherent current limiting capability to improve the stability and transient response characteristics of the system, which can effectively solve the problem that the steady-state error and the reference current reference value appearing in the SMC converter are difficult to measure. The current inner loop adopts the SMC strategy, which has the advantage of fast dynamic response speed, and realizes automatic tracking of the reference voltage [13].

#### 3.2. Design of the sliding mode control rate

Sliding mode control is especially suitable for variable structure systems with strong robustness and fast dynamic response [14]. The beam supply phase-shift full-bridge converter continuously switches the on and off states of the switch tube, which is a strictly variable structure system, which is highly compatible with the principle of sliding mode variable structure control. Therefore, sliding mode variable structure control is particularly suitable for beam supply to achieve good robustness and transient characteristics. SMC is divided into two stages of arrival and sliding [15]. Let the switching function be:

$$s = k_1 x_1 + k_2 x_2 + k_3 x_3 = J^T x, \quad (11)$$

where:  $J^T = [k_1 \ k_2 \ k_3]$ ,  $k_1, k_2, k_3$  both are positive sliding coefficients.

Let  $u$  be the sliding mode control rate:

$$u = u_{eq} + u_{sw}, \quad (12)$$

where:  $u_{eq}$  is the equivalent control rate,  $u_{sw}$  is the switching control rate. When  $s \neq 0$ , the system is in the arrival phase, and the sliding mode control rate is the switching control  $u_{sw}$ :

$$u_{sw} = \frac{1}{2} (1 + \text{sign}(s)) = \begin{cases} 1 & s > 0 \\ 0 & s < 0 \end{cases}. \quad (13)$$

When  $s = 0$ , the system is in the sliding phase, and the control rate is the equivalent control rate  $u_{eq}$ . Deriving  $s$  to make it equal to zero, that is  $\dot{s} = 0$ , which can be obtained by (10), (13):

$$u_{eq} = \frac{1}{nV_{in}} \left( \frac{L_f}{RC_f} + R_d - \frac{k_1}{k_2} L \right) i_c + \frac{1}{V_{in}} \left( \frac{R_d}{R} + 1 \right) v_o + \frac{L_f C_f k_3}{nV_{in} k_2} (V_{ref} - v_o), \quad (14)$$

where,  $i_c = C\dot{v}_o$ .

The system control rate can be written as:

$$u = \begin{cases} 1 & s > 0 \\ u_{eq} & s = 0 \\ 0 & s < 0 \end{cases} \quad (15)$$

According to comprehensive Formulas (5)–(14), when  $u = 1$  or  $u = 0$ , the motion trajectory of the system from an arbitrary initial position  $(x_1, x_2, x_3)$  in the state space, the phase trajectory of the substructure is as shown in Fig. 7.

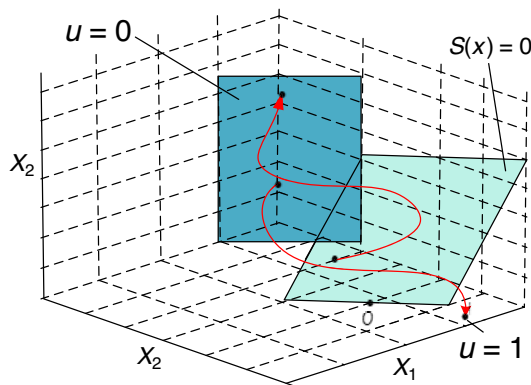


Fig. 7. Substructure phase trajectory motion diagram

The constraint of the sliding coefficient only provides general information about the existence of the sliding mode [16], but does not give the relationship between the performance of the converter and the sliding coefficient, nor does it give general information on the selection of parameters. When the system is in the sliding mode area:

$$k_1 x_1 + k_2 \frac{dx_1}{dt} + k_3 \int x_1 dt = 0. \quad (16)$$

Put the above formula into the standard second-order system form:

$$\frac{d^2 x_1}{dt^2} + 2\xi^2 \omega_n \frac{dx_1}{dt} + \omega_n^2 x_1 = 0, \quad (17)$$

where:  $\omega_n = \sqrt{(k_3/k_2)}$  is an undamping natural frequency,  $\xi = (\alpha_1/2\sqrt{k_3 k_2})$  is the damping coefficient. Rearrange the above equations into:

$$\frac{k_3}{k_2} = \frac{1}{4\xi^2} \left( \frac{k_1}{k_2} \right)^2. \quad (18)$$

In linear second-order systems [17], there are three possible types of response: underdamped, critically damping, overdamped. The system only meets the requirements for critical damped:

When  $\xi = 1$ , the system is in critical damping state [18]. At this time, if the system is in slip mode, the following output voltage error expression is:

$$x_1(t) = (\lambda_1 + \lambda_2 t) e^{-\xi \omega_n t} \geq 0, \quad (19)$$

where,  $A_1$  and  $A_2$  are determined by initial conditions.

Since the decay rate of response is determined by the factor  $\xi \omega_n$ , decay time constant is:

$$\tau = \frac{1}{\omega_n} \sqrt{\frac{k_2}{k_3}}. \quad (20)$$

If  $\xi = 1$ , substituting (18) into (20) gives:

$$\tau = 2 \frac{k_2}{k_1}. \quad (21)$$

Suppose the system needs 2 times the decay time, that is,  $2\tau$  seconds to reach the steady-state. The required sliding coefficient ratio is:

$$\frac{k_1}{k_2} = \frac{4}{T_s}, \quad \frac{k_3}{k_2} = \frac{4}{T_s^2}. \quad (22)$$

### 3.3. Accessibility condition analysis

The sliding mode controller includes the selection of the switching function and the determination of the SMC rate, so that the system satisfies the three basic elements of the sliding mode control, the sliding mode reachability, and the sliding mode motion stability [19].

#### a. Meet the arrival conditions

To verify the arrival condition, it is only necessary to ensure that has a decreasing trend when switching functions, and  $s$  has an increasing tendency when switching functions. The size of the switching function  $s$  is determined, and in the arrival phase, it is in a dominant role, and the other values are all positive values, so the size of the switching function  $s$  is determined. If the output voltage is lower than the reference voltage, at this time, the control rate is reflected on the circuit to turn on the power switch, and the output voltage rises. Similarly, if the output voltage is higher than the reference voltage, the switching function and the control rate are displayed on the circuit to turn off the power switch and the output voltage drops. From this analysis, the switching control rate  $u$  can be obtained. The arrival control condition is satisfied, and the handover control rate can be expressed as:

$$u_{sw} = \begin{cases} 1 & s > 0 \\ 0 & s < 0 \end{cases}. \quad (23)$$

#### b. Satisfy the existence condition

When the switching control rate is determined, the following is to ensure that the sliding coefficient and the condition of the sliding surface are satisfied. The correct approach is to verify the local reachability conditions of the system state trajectory:

$$\lim_{s \rightarrow 0} s \cdot \dot{s} < 0. \quad (24)$$

From Equations (14) and (24), we can get:

$$0 < \left[ \frac{k_1}{k_2} - \frac{1}{L_f C_f} \left( \frac{L}{R} + R_d C_f \right) \right] x_2 + \left[ \frac{k_3}{k_2} - \frac{1}{L_f C_f} \left( \frac{R_d}{R} + 1 \right) \right] x_1 + \frac{1}{L_f C_f} \left( \frac{R_d}{R} + 1 \right) V_{\text{ref}} < < \frac{nV_{\text{in}}}{L_f C_f} k_2. \tag{25}$$

The sliding coefficient of the system must satisfy the above formula.

### 3.4. Dual-mode switching control

The system has a dual-mode working mode, that is, a phase-shift mode and a duty ratio working mode, which are determined according to the actual load demand of the system. When the upper machine issues a working condition command, the dual-mode is freely switched, and Fig. 8 is a mode switching state diagram.

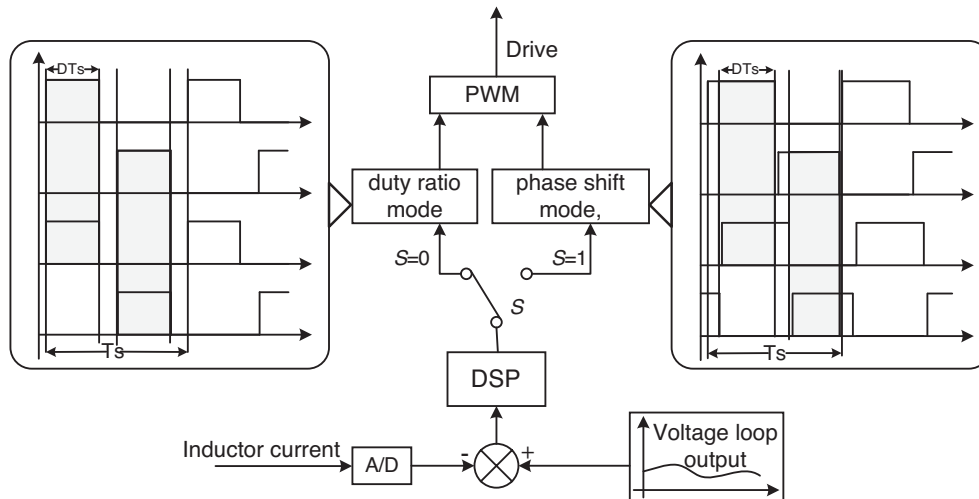


Fig. 8. System switching control chart

After the beam supply is completed, it enters the phase-shift mode, and then determines whether the phase-shift mode is switched to the duty ratio mode according to the load output voltage. When the load output voltage is less than 1000 V, the duty ratio mode is switched by the phase-shift mode, which is greater than 1000 V. The system works in phase-shift mode. The output signal mode is the output of the mode switching,  $s = 1$  indicates the phase-shift mode, and  $s = 0$  indicates the duty ratio mode [20].

## 4. Simulation analysis

To verify the correctness of the proposed control strategy, the simulation model of the system was built in MATLAB/Simulink. The parameters of the converter are shown in Table 1. The system

has been verified by simulation experiments under a purely resistive rated load. The simulation results are compared with the classic PID control.

Table 1. The parameters of full bridge converter

Parameter name	Symbol	Value	Unit
Input DC voltage	$V_{in}$	100	V
Transformer ratio	$K$	1/10	
Load resistance	$R$	200	$\Omega$
Filter inductor	$L_f$	150	$\mu\text{H}$
$T$ leakage inductance	$L_r$	18	$\mu\text{H}$
Filter capacitor	$C_f$	12	$\mu\text{F}$
Switching frequency	$f_s$	50	kHz
Feedback control rate	$c_1$	$1 \times 10^6$	

In Fig. 9 the red line and black line respectively, indicate the output voltage of the system using sliding mode control and traditional voltage and current multiple closed-loop control in phase-shift mode. At this time, the converter operates under current continuous mode (CCM), and the input and output DC voltages are 100 V and 1800 V. The frequency is 50 kHz. It can be seen from the figure that the settling time is about 8 ms by the sliding mode control, and the settling time is about 10 ms by the traditional multiple closed-loop control. It can be concluded that the sliding mode control has a short settling time, and the system has basically no overshoot, and has good performance.

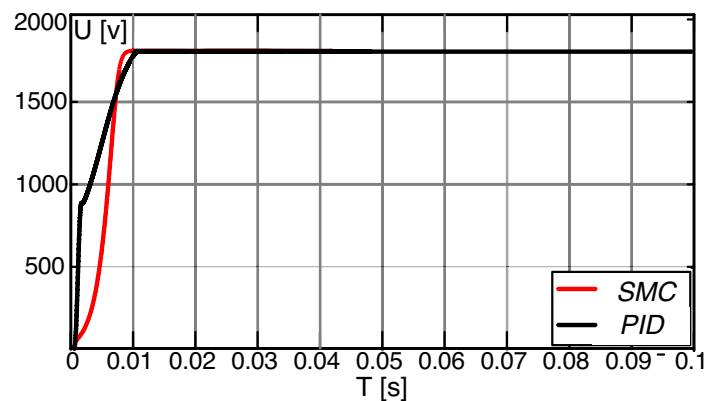


Fig. 9. SMC and PID control output voltage

The abnormal working condition experiment of the converter is performed and the voltage reference value and the load are abruptly changed. The red line in Fig. 10 shows the output curve

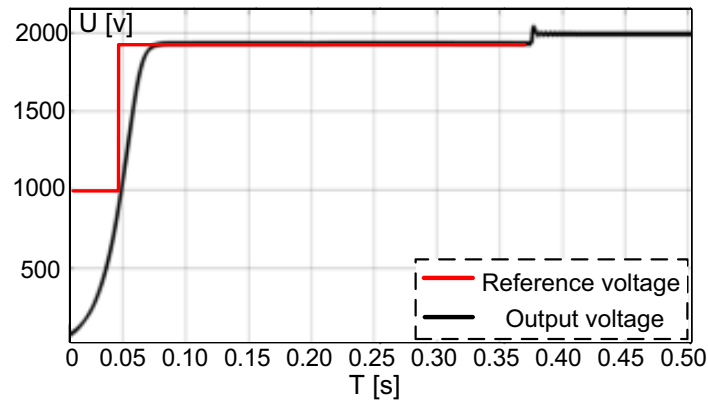


Fig. 10. Abrupt reference voltage output voltage (SMC)

from the initial given 1000 V rise to 1800 V when the system is running at 0.05 s and suddenly changes the given voltage (SMC). In addition the black line shows a sudden change in the given voltage, rising from the initial given 1000 V to 1800 V, and the system output voltage is as shown. After 2.5 ms the system tends to be stable.

To verify the robust performance of the designed sliding-mode controller furtherly, the simulation of sudden load increase and decrease is carried out. As shown in Fig. 11 and Fig. 12, the load resistance is suddenly reduced at 0.25 s and the system tends to be stable gradually within the settling time about 4 ms. Although the output voltage has a certain degree of pulsation, the voltage is stabilized quickly. Because the converter adopts SMC, the system has strong robustness and certain anti-disturbance performance and can satisfy the actual demand of high-performance ion thruster.

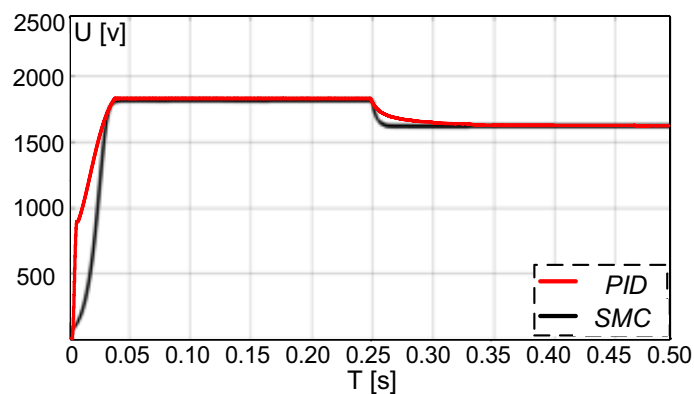


Fig. 11. Output voltage under sudden load decrease

As shown in Fig. 13 and Fig. 14, the load resistance is suddenly increased at 0.25 s. From the output voltage and current curve, it can be concluded that the settling time is about 4 ms and the

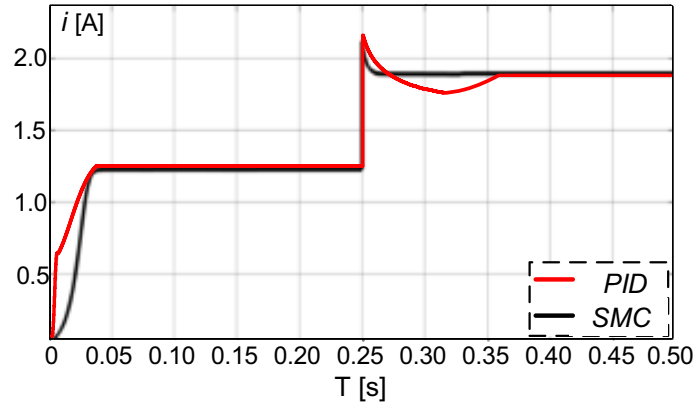


Fig. 12. Output current under sudden load decrease

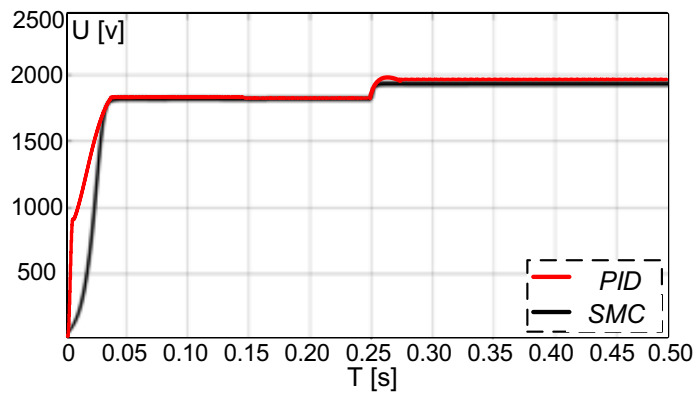


Fig. 13. Output voltage under sudden load increase

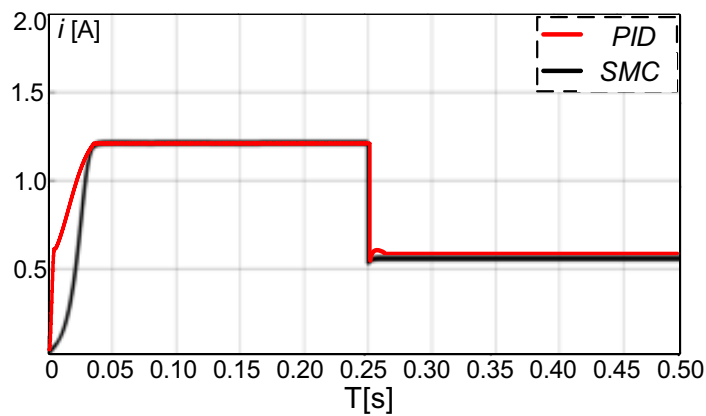


Fig. 14. Output current under sudden load increase

system becomes stable gradually. The system has strong dynamic response characteristics and anti-interference performance.

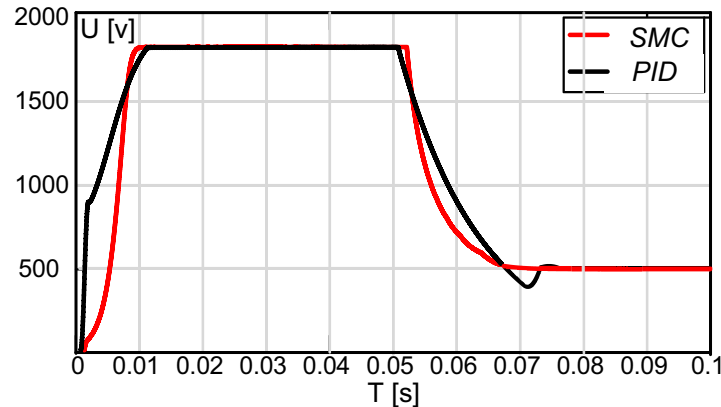


Fig. 15. Comparison between SMC and PID control

As shown in Fig. 15, the red line indicates the output voltage when the system switches to the PWM mode from the phase-shift control with sliding-mode. The black line indicates the output voltage when the system switches to the PWM mode from the phase-shift mode with dual closed-loop PID control. The comparison shows that the switching of SMC is relatively smooth and the generated shaking is small. The actual effect is good.

## 5. Conclusion

Compared with the traditional PID control strategy, the improved sliding mode control strategy in the DC/DC converter of beam supply has good dynamic quality and a certain practical application value. the SMC can be used to make the mode switching smoother. The generated shaking is small and the actual effect is better. The simulation experiment of abnormal working conditions shows that the designed sliding-mode controller effectively solves the problem of the output voltage affected by load variation and input voltage fluctuation. The output voltage area has a small steady-state error controller and can quickly track the reference signal. The system has strong robustness and achieves output constant voltage control.

## References

- [1] Ma S., Wei G., Li Y., *Design of power supply test unit for electric propulsion system thruster*, Vacuum and Cryogenics (2017).
- [2] Wang S., Wang Wei, *Design of a 5kW Modular Power Processing Unit for 30cm Ion Thruster*, Spacecraft Engineering, vol. 22, no. 5, pp. 74–79 (2013).
- [3] Li F., Kang Q., Qing J., Li Y., *Technology for power processing unit used in high power electric propulsion*, Journal of Beijing University of Aeronautics and Astro, vol. 42, no. 8, pp. 1575–1583 (2016).

- [4] Wu T., Zhai H., Wu R., *Simulation and Analysis of Beam Supply for High Power Ion Thruster Based on Saber*, Space Electronic Technology (2017).
- [5] Kurokawa F., Murata K., Yoshida R. *et al.*, *A novel P-I-D digital control FPGA for a switching power supply in HVDC system*, IEEE International Symposium on Power Electronics for Distributed Generation Systems (2012), DOI: 10.1109/PEDG.2012.6254051.
- [6] Arvind S., Akshay R., Sreedevi A., *A novel constant frequency sliding mode control of DC-DC converters*, 2016 IEEE 7th Power India International Conference (PIICON), IEEE (2016), DOI: 10.1109/POWERI.2016.8077387.
- [7] Gao Ming, Wang Dazhi, Li Zhao, *A PWM Full Order Robustness Sliding Mode Control for Phase-Shifted Full-Bridge Converter*, Transactions of China Electrotechnical Society, vol. 33, no. 10, pp. 2293–2302 (2018).
- [8] Hussainy S.A.A., Tandon R.G., Kumar S., *PWM Based Sliding Mode Control of DC-DC converters*, International Conference on Advances in Power Conversion and Energy Technologies (2012), DOI: 10.1109/APCET.2012.6302052.
- [9] Lopez-Santos O., Martinez-Salamero L., Garcia G. *et al.*, *Efficiency analysis of a sliding-mode controlled quadratic boost converter*, Power Electronics Iet, vol. 6, no. 2, pp. 364–373 (2013).
- [10] Yao X., Sun Y., *Sliding mode control of DC-DC buck converter based on hysteresis modulation*, IEEE Conference and Expo Transportation Electrification Asia-Pacific (ITEC Asia-Pacific) (2014), DOI: 10.1109/ITEC-AP.2014.6940728.
- [11] Jiao S., Zhang L., Liu D., *Fuzzy Sliding Mode Control of High Frequency Switching Power Supply Based on Incremental Switch Item*, Transactions of China Electrotechnical Society, vol. 33, no. 22, pp. 5311–5318 (2018).
- [12] Jiao S., Liu C., Huang W., *Fuzzy Sliding Mode Control of High Frequency Switching Power Supply Based on Discrete-Time Variable Rate Reaching Law*, Transactions of China Electrotechnical Society, vol. 30, no. 20, pp. 108–117 (2015).
- [13] Wang D., Li B., *Research on Sliding Mode Algorithm for Buck Converter*, Microelectronics, vol. 47, no. 04, pp. 557–561 (2017).
- [14] Knight J., Shirsavar S., Holderbaum W., *An improved reliability cuk based solar inverter with sliding mode control*, IEEE Transactions on Power Electronics, vol. 21, no. 4, pp. 1107–1115 (2017).
- [15] Alsmadi Y.M., Utkin V., Hajahmed M.A. *et al.*, *Sliding mode control of power converters: DC/DC converters*, International Journal of Control, vol. 6, pp. 1–22 (2017).
- [16] Na W., Chen P., Singh H. *et al.*, *Multi-phase sliding mode control for chattering suppression in a DC-DC converter*, Energy Conversion Congress and Exposition (2017), DOI: 10.1109/ECCE.2016.7855284.
- [17] Cucuzzella M., Lazzari R., Trip S. *et al.*, *Sliding mode voltage control of boost converters in DC microgrids*, Control Engineering Practice, vol. 73, pp. 161–170 (2018).
- [18] Repecho V., Biel D., Olm J.M. *et al.*, *Robust sliding mode control of a DC/DC Boost converter with switching frequency regulation*, Journal of the Franklin Institute, vol. 355, iss. 13, pp. 5367–5383 (2018).
- [19] Pichan M., Rastegar H., *Sliding Mode Control of Four-Leg Inverter with Fixed Switching Frequency for Uninterruptible Power Supply Applications*, IEEE Transactions on Industrial Electronics, vol. 64, no. 3, pp. 6805–6814 (2017), DOI: 10.1109/TIE.2017.2686346.
- [20] Aroudi A.E., Martinez B., Calvente J., *Sliding-mode control of a boost converter feeding a buck converter operating as a constant power load*, International Conference on Green Energy Conversion Systems (2017), DOI: 10.1109/GECS.2017.8066249.